Chapter 1

CONCLUSION

1.1 Summary of Results

The results presented in this dissertation represent the best limits to date for each ^{76}Ge $\beta\beta$ E.S. decay mode. Meaningful constraints are placed on the value of the $\beta\beta$ E.S. to the 0_1^+ nuclear matrix element. This chapter will place the results of this analysis in the context of previous results and theoretical predictions. It will also discuss the potential for future improvements on this result.

1.1.1 Comparison to GERDA Phase I result

GERDA phase I published the previous best results for all $2\nu\beta\beta$ decay modes in 2015, using 22.3 kg-y of exposure[1]. This result, using 21.3 kg-y of exposure has achieved a significantly higher sensitivity and limit. GERDA employed similar analysis techniques to this result, but the MAJORANA DEMONSTRATOR enjoys several advantages in performing searches in multi-site detectors. First, the GERDA liquid argon veto acts as shielding for γs that travel between HPGe detectors. A 600 keV γ has a mean free path through liquid argon of $\sim$9 cm, and the spacing between different GERDA strings is several cm, resulting in significantly lower detection efficiency compared to the MAJORANA DEMONSTRATOR. For the decay to the 0_1^+ state, GERDA had a detection efficiency of 0.989 %, while the MAJORANA DEMONSTRATOR had an efficiency of 1.71%, exposure-averaged between the two modules.

In addition, GERDA has a significantly higher background rate in the ROI: for the decay to the 0_1^+ state, GERDA expects 7.9 background counts while the MAJORANA DEMONSTRATOR expects 2.02 counts. One reason for this, is that the MAJORANA DEMONSTRATOR has significantly better resolution: the FWHM for a 583 keV coincident γ is 1.3 keV for the

Table 1.1: A comparison between the key parameters behind the results for MAJORANA DEMONSTRATOR and GERDA for each $2\nu\beta\beta$ to excited states mode. Backgrounds and efficiencies are combined across modules and peaks. Limits and sensitivities are at 90% Neyman confidence level.

	MAJORANA (21.3 kg)				GERDA (22.3 kg-y)			
$2\nu\beta\beta$ E.S.	Exp.	Eff.	Limit	Sensitivity	Exp.	Eff.	Limit	Sensitivity
Decay Mode	BGs	(%)	(10^{23} y)	(10^{23} y)	BGs	(%)	(10^{23} y)	(10^{23} y)
$0^+_{g.s.} \xrightarrow{2\nu\beta\beta} 0^+_1$	2.02	1.71	> 6.8	> 7.0	7.9	0.919	> 3.7	> 1.9
$0^+_{g.s.} \xrightarrow{2\nu\beta\beta} 2^+_1$	0.72	1.06	> 9.6	> 5.3	2.4	0.389	> 1.6	> 1.3
$0^+_{g.s.} \xrightarrow{2\nu\beta\beta} 2^+_2$	3.40	1.64	> 5.6	> 5.3	8.7	0.686	> 2.3	> 1.4

MAJORANA DEMONSTRATOR, and 4.2 keV for GERDA. Electronic crosstalk in the GERDA detector array increases the FWHM from 3.8 keV to 4.2 keV. The LMFE boards (Section **??**) and their proximity to the MAJORANA detectors provide low noise and minimal crosstalk (Section **??**), and the charge trapping correction (Section **??**) provides further improvements. As a result, the MAJORANA DEMONSTRATOR uses separate ROIs for the 559 and 563 keV γs that combine to a width of 3.3 keV, while GERDA uses a single 8.5 keV wide ROI. This explains most of the difference in background rates between the experiments; if GERDA had the same ROI, the expected background rate would reduce to 3.1 counts. Additionally, the dominant background for GERDA in this search comes from ^{42}K from the ^{42}Ar-^{42}K-^{42}Ca chain inside of the liquid argon shield (see Figure 1.1). Because this decay can emit γs from the interior of the detector array, it will produce multi-site events with high enough energies to pass the coincident energy cuts at a relatively high rate. This likely explains the remaining difference between the background rates.

Since publishing the phase I result[1], GERDA has implemented numerous improvements that may improve on the previous result[2]. GERDA phase II has since replaced many coaxial

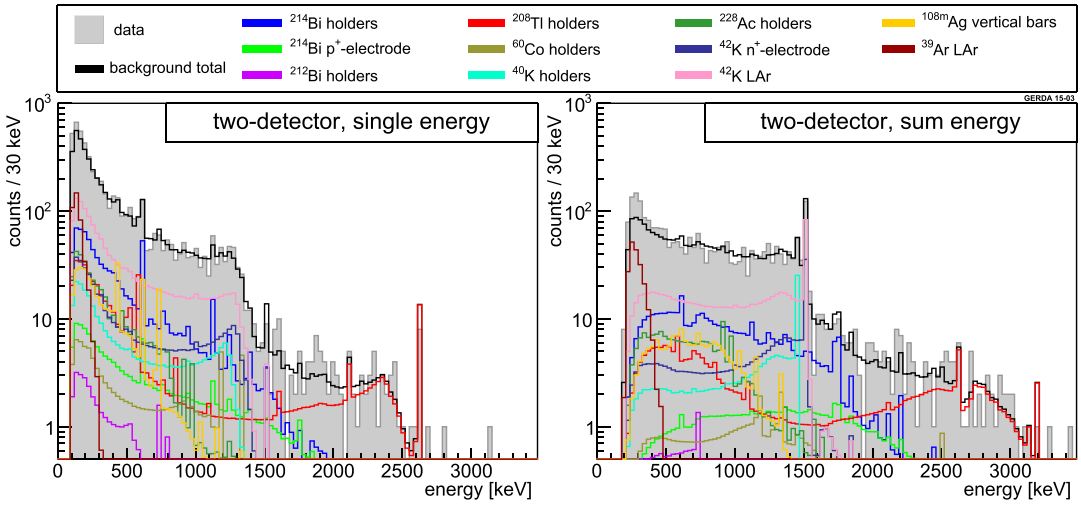

Figure 1.1: The measured GERDA single-hit and sum-energy spectra for high multiplicity events compared with the measured data. The dominant background in this spectrum originates from ^{42}K in the liquid argon shield. Taken from [1].

HPGe detectors with BEGe detectors, which are smaller, resulting in a more granular array that will be more sensitive to multi-detector events. Additionally, the liquid argon shield has been instrumented, enabling it to act as an active shield, which may reduce backgrounds, and potentially could be used to detect γs from the excited state decays. ^{42}K backgrounds are expected to be reduced with the addition of protective shrouds around detectors. Finally, improvements to the signal electronics and corrections for detector crosstalk may be implemented to improve the energy resolution.

1.1.2 Comparison to Theoretical Predictions

Section **??** and table **??** presented various half-life calculations for the $2\nu\beta\beta$ to excited state decay modes and discussed some of the factors that lead to an uncertainty spanning orders of magnitude in half-life. Because of the large number of factors that affect these calculations, it is difficult to draw conclusions about the different models based on a comparison

to an experimental result. Nevertheless, we shall perform such a comparison: the 90% limit presented in this document rules out all predictions made with QRPA-based models for the $2\nu\beta\beta$ to 0_1^+ state (the largest prediction by Suhonen[1], calculated assuming a g_A factor of 1.27, is disfavored with a p-value of 0.08). For the $2\nu\beta\beta$ to 2_1^+ state the HFB prediction by Dhiman and Raina[3] is newly ruled out. The $2\nu\beta\beta$ to 2_2^+ state remains firmly out of reach of experiments. For the $0\nu\beta\beta$ decay modes, a meaningful comparison between experiment and nuclear theory calculations is not possible until the $0\nu\beta\beta$ to the ground state is observed. In addition, it is difficult to predict how an error in the prediction of any $2\nu\beta\beta$ to excited state half-life might correlate with an error in the $0\nu\beta\beta$ half-life predictions, for reasons discussed in Section **??**. Improvements in some of the existing models presented in Table **??** and future models can use excited state results as an additional test. Ideally, they will agree with a measured result of the excited state decay half-lives, and predict similar values of the $0\nu\beta\beta$ nuclear matrix elements, with measurements across multiple isotopes. Table 1.2 shows the current status of searches for $2\nu\beta\beta$ to 0_1^+ states across multiple isotopes. For a more complete discussion, see Barabash's review [4].

1.2 The Future of $\beta\beta$ E.S. in ^{76}Ge

The MAJORANA DEMONSTRATOR has been continuously acquiring data since the April 18, 2018 cutoff used in this analysis, and will continue to do so until it has a projected ∼100 kg-y of exposure. In addition, much of the data-taking period remains to be unblinded, which increases the available exposure before the cutoff to ∼40 kg-y. This increase in exposure should increase the sensitivity to the $\beta\beta$ E.S. to the 0_1^+ state half-life above 10^{24} y, potentially enabling a test of the EFT prediction of $1.7 \cdot 10^{24}$ y[8].

1.2.1 Potential Improvements

In addition to gathering additional exposure, other improvements to this search are possible. In particular, the AvsE parameter, which is used to determine whether a waveform within a single detector is multi-site or single-site (see Section **??**), may be useful. When a γ is

Table 1.2: Table of results and predictions for the half-life of $2\nu\beta\beta$ to 0_1^+ states across multiple isotopes. For the RQRPA results, half-lives were calculated within the references; for the IBM and EFT results, they were calculated using equation **??**.

	Experiment	Theoretical $T_{1/2}^{2\nu\ E.S.}$ (y)		
Isotope	$T_{1/2}^{2\nu\ E.S.}$ (y)	RQRPA[5, 6]	IBM[7]	EFT[8]
^{48}Ca	$> 1.5 \cdot 10^{20}$ [9]	-	$2.0 \cdot 10^{23}$	-
^{76}Ge	$> 6.8 \cdot 10^{23}$	$(1.0 - 3.1) \cdot 10^{23}$	$7.1 \cdot 10^{24}$	$1.7 \cdot 10^{24}$
^{82}Se	$> 3.4 \cdot 10^{22}$ [10]	$(1.5 - 3.3) \cdot 10^{21}$	$4.1 \cdot 10^{23}$	$4.5 \cdot 10^{22}$
^{96}Zr	$> 3.1 \cdot 10^{20}$ [11]	$(2.4 - 3.8) \cdot 10^{21}$	$3.0 \cdot 10^{24}$	-
^{100}Mo	$6.7^{+0.5}_{-0.4} \cdot 10^{20}$ [4]	$(0.81 - 4.1) \cdot 10^{22}$	$5.7 \cdot 10^{21}$	$5.2 \cdot 10^{20}$
^{116}Cd	$> 2.0 \cdot 10^{21}$ [12]	$(1.6 - 3.3) \cdot 10^{24}$	$8.4 \cdot 10^{23}$	$1.8 \cdot 10^{23}$
^{130}Te	$> 2.5 \cdot 10^{23}$ [13]	$(7.2 - 16) \cdot 10^{23}$	$3.0 \cdot 10^{25}$	$2.8 \cdot 10^{25}$
^{136}Xe	$> 8.3 \cdot 10^{23}$ [14]	$(1.3 - 8.9) \cdot 10^{23}$	$3.0 \cdot 10^{25}$	-
^{150}Nd	$1.2^{+0.3}_{-0.2} \cdot 10^{20}$ [4]	-	$1.9 \cdot 10^{21}$	-

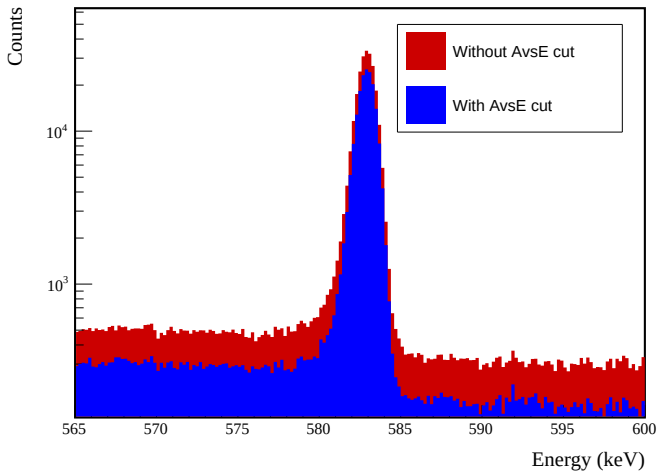

Figure 1.2: A 583 keV peak from a ^{228}Th calibration run using AvsE to select multi-site events (blue). The effect is to keep 75% of events in the peak while keeping only 41% of events in the continuum.

fully absorbed within a single detector, it will typically be detected as a multi-site event, while most Compton continuum events are single-site. For example, the 583 keV γ from the ^{228}Th spectrum is $\sim$75% multi-site, while the Compton continuum is only $\sim$41% multi-site, as shown in Figure 1.2. If the peak search were to only look at multi-site events, it would likely produce a small gain of up to $\sim$20% in sensitivity.

The coincident energy cut could also benefit from using AvsE. For decay modes with only a single γ (such as the 2_1^+ modes), the coincident detector in a true signal will have only a single site, from the $\beta\beta$-decay. On the other hand, for events with multiple γs, coincident events with energy above the Q-value of the decay will result from events involving the internal absorption of one of the γs; as a result, these events will be inherently multi-site. Using AvsE in this cut will be especially important for differentiating between 2_1^+ and 0_1^+ events since they both involve a 559 keV peak. This means that some method of differentiating between events involving one and two γs will be critical to differentiating

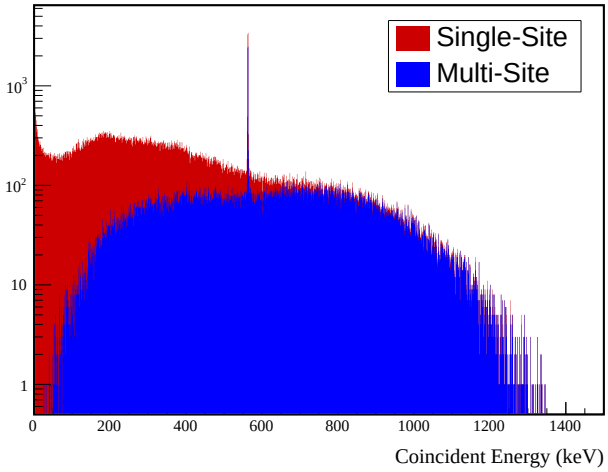

Figure 1.3: Simulated energy spectrum for hits in coincidence with a 559 or 563 keV γ from a $2\nu\beta\beta$ to 0_1^+ event. The dt-heuristic was applied to simulate the effect of an AvsE cut.

events in this peak, and AvsE may provide the best way of doing so. A simulation of the effect of AvsE on the coincident energy spectrum is shown in Figure 1.3. The reason AvsE is not currently used for this search is that it cannot be simulated reliably. The current method of simulating this parameter, called the dt-heuristic, is calibrated over an energy range close to 2039 keV, and has a relatively high error at the energies of interest for this analysis. Since this analysis relies heavily on uncertain simulations that would introduce significant systematic error, and since the improvements brought by using AvsE are expected to be small, this cut was not used for this analysis. However, further improvements to the dt-heuristic and development of pulse-shape simulations that can improve AvsE simulation may allow the implementation of this cut in the future.

1.2.2 Multi-Site Event Decomposition

In addition to distinguishing between single- and multi-site events, PPC HPGe detectors offer the possibility to decompose a multi-site waveform and measure the energies of the

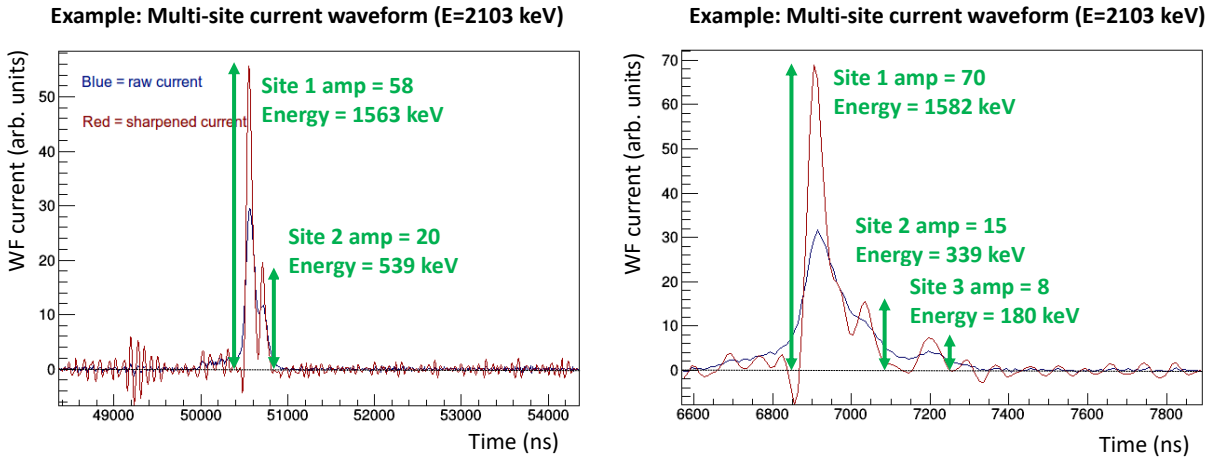

Figure 1.4: A Wiener deconvolution of two current waveforms with a Lorentzian deconvolution kernel. The current peaks can be identified and their amplitudes calibrated to measure energy. The waveforms were selected from the SEP and are expected to have a site with 1592 keV of energy.

component sites. Multi-site waveforms consist of multiple rises, as discussed in Section **??**, and the current amplitude of each individual rise is proportional to the energy contained in the local charge cloud producing it. This proportionality is the reason the AvsE parameter works: for a single-site, the maximum current amplitude should be some fixed fraction of the total energy, while for multi-site waveforms, the current amplitude will be significantly less. Due to electronic noise, however, picking out individual components of waveforms and measuring the energy with each one is difficult. One method that has been demonstrated for doing this is to apply a Wiener deconvolution filter, which uses deconvolution with a known kernel function in order to sharpen the current peaks, combined with an optimal Wiener filter to prevent noise from blowing up. A proof of principle for this technique is shown in Figure 1.4.

To demonstrate the effectiveness of this technique, we can look at an inherently multi-site event such as a single-escape event. The single-escape peak produced by the ^{208}Tl

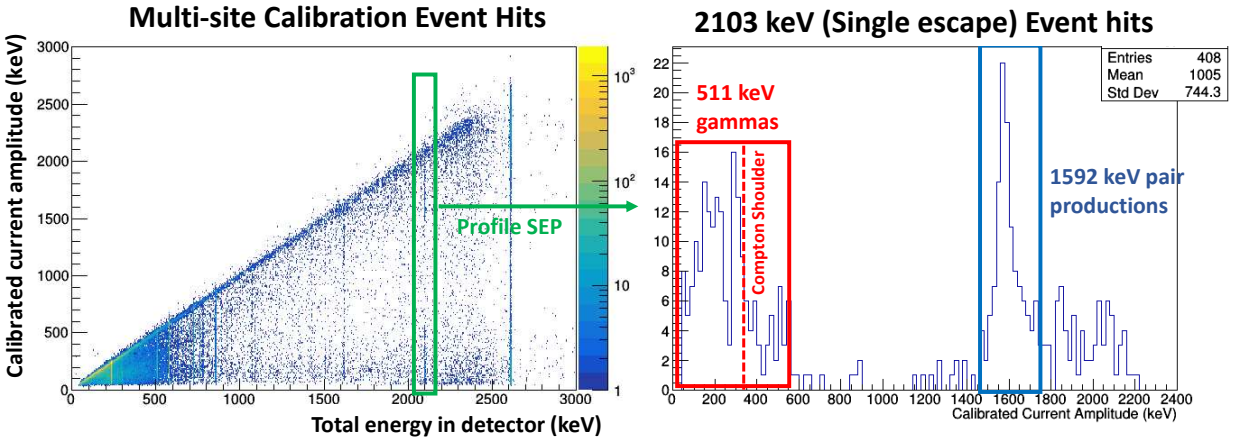

Figure 1.5: Left: A 2D spectrum showing the energy of individual sites in multi-site events from a ^{228}Th calibration run, vs the total energy of the event.
Right: A profile along the single escape peak (total energy 2103 keV). The expected features of a 1592 keV peak for the pair production site and a 511 keV Compton spectrum from the γ are observable.

2614 keV γ will consist of a 1592 keV pulse, produced by the site of the pair production, and additional sites that sum to 511 keV, produced by the annihilation γ. Figure 1.5 shows how these expected features can be extracted from SEP events in a MAJORANA DEMONSTRATOR calibration run. Using this technique, we are able to identify the 1592 keV site in 44% of SEP events, a number that could significantly improve with refinements to the algorithm.

Multi-site event decomposition would be useful in searching for $\beta\beta$ E.S. events because these events are inherently multi-site. The search presented here takes advantage of this by looking at multi-detector events; however, often the γ-rays in these events will not escape the source detector without losing at least some energy. In this case, the event would not be visible using this search's detection signature, but would be visible by looking for individual sites that sum to the full γ energy. Based on simulations, 60% of $2\nu\beta\beta$ to 0_1^+ events have the full energy of at least one of the two γs absorbed inside of Germanium detectors, which sets a much higher ceiling on the detection efficiency than the 2% used in this document. Using

the 44% of pair production sites tagged in SEP events as a proxy, it is imaginable that such a search could achieve a detection efficency of 20-25%, a ten-fold improvement over the current search. This would also increase the measured background rate significantly, by introducing single-detector multi-site backgrounds; furthermore, the poorer energy resolution for these events would necessitate a wider ROI. Even so, this could produce a large gain in sensitivity.

1.2.3 Searching for $\beta\beta$ E.S. with LEGEND

LEGEND-200 is preparing to begin operation in 2021, with lower backgrounds than the MAJORANA DEMONSTRATOR and GERDA and a target exposure of ∼1 t-y (Section **??**). In spite of this high exposure, however, many challenges remain for LEGEND-200 to offer a significantly improved result in the search for $\beta\beta$ E.S.. LEGEND-200 will use the GERDA liquid argon shield, which carries disadvantages for a $\beta\beta$ E.S. search due to higher backgrounds and lower detection efficiencies. GERDA Phase II may find techniques to mitigate these disadvantages, and will likely publish a result soon. In addition, LEGEND-200 is using the inverted coaxial detector geometry, which increases the mass of each detector, but as a result reduces the granularity of the detector array. This will further reduce detection efficiency. Finally, once the $\beta\beta$ E.S. to the 0_1^+ decay is discovered, it will act as the largest background for the 2_1^+ decay, which will further limit sensitivity without finding a method to distinguish the two. For these reasons, LEGEND-200 may struggle to significantly improve upon the final MAJORANA DEMONSTRATOR results without implementing many of the improvements mentioned in the previous section.

If LEGEND-200 succeeds in these improvements and manages a measurement with $> 10\%$ detection efficiency that remains nearly background free, future measurements could feasibly have half-life sensitivities exceeding 10^{26} y. This would almost certainly observe the $\beta\beta$ E.S. to 0_1^+ decay mode (and if it didn't that would be an interesting result in its own right!). It would also begin to probe into the theoretical half-life predictions for the 2_1^+ decay mode, with potentially interesting results regarding a Bosonic component of neutrinos (Section **??**, [15]). With the same improvements and lower backgrounds, LEGEND-1000 may probe half-

lives exceeding 10^{27} y, offering a strong possibility of observing $2\nu\beta\beta$ to the 2_1^+ excited state. Finally, under the optimistic scenario that LEGEND-200 discovers $0\nu\beta\beta$, LEGEND-1000 may begin a search for $0\nu\beta\beta$ to excited states, with implications toward understanding the underlying mechanism for $0\nu\beta\beta$ decay and the Majorana nature of neutrino mass.

BIBLIOGRAPHY

[1] M Agostini et al. $2\nu\beta\beta$ decay of 76ge into excited states with GERDA phase i. *Journal of Physics G: Nuclear and Particle Physics*, 43(4):044001, sep 2015.

[2] GERDA Collaboration, M. Agostini, A. M. Bakalyarov, M. Balata, I. Barabanov, L. Baudis, C. Bauer, E. Bellotti, S. Belogurov, S. T. Belyaev, G. Benato, A. Bettini, L. Bezrukov, T. Bode, D. Borowicz, V. Brudanin, R. Brugnera, A. Caldwell, C. Cattadori, A. Chernogorov, V. D'Andrea, E. V. Demidova, N. Di Marco, A. Domula, E. Doroshkevich, V. Egorov, R. Falkenstein, N. Frodyma, A. Gangapshev, A. Garfagnini, P. Grabmayr, V. Gurentsov, K. Gusev, J. Hakenmüller, A. Hegai, M. Heisel, S. Hemmer, R. Hiller, W. Hofmann, M. Hult, L. V. Inzhechik, L. Ioannucci, J. Janicskó Csáthy, J. Jochum, M. Junker, V. Kazalov, Y. Kermaïdic, T. Kihm, I. V. Kirpichnikov, A. Kirsch, A. Kish, A. Klimenko, R. Kneißl, K. T. Knöpfle, O. Kochetov, V. N. Kornoukhov, V. V. Kuzminov, M. Laubenstein, A. Lazzaro, V. I. Lebedev, B. Lehnert, M. Lindner, I. Lippi, A. Lubashevskiy, B. Lubsandorzhiev, G. Lutter, C. Macolino, B. Majorovits, W. Maneschg, E. Medinaceli, M. Miloradovic, R. Mingazheva, M. Misiaszek, P. Moseev, I. Nemchenok, S. Nisi, K. Panas, L. Pandola, K. Pelczar, A. Pullia, C. Ransom, S. Riboldi, N. Rumyantseva, C. Sada, F. Salamida, M. Salathe, C. Schmitt, B. Schneider, S. Schönert, J. Schreiner, A-K. Schütz, O. Schulz, B. Schwingenheuer, O. Selivanenko, E. Shevchik, M. Shirchenko, H. Simgen, A. Smolnikov, L. Stanco, L. Vanhoefer, A. A. Vasenko, A. Veresnikova, K. von Sturm, V. Wagner, A. Wegmann, T. Wester, C. Wiesinger, M. Wojcik, E. Yanovich, I. Zhitnikov, S. V. Zhukov, D. Zinatulina, A. J. Zsigmond, K. Zuber, and G. Zuzel. Upgrade for phase ii of the gerda experiment. *The European Physical Journal C*, 78(5):388, May 2018.

[3] S. K. Dhiman and P. K. Raina. Two-neutrino double-beta decay matrix elements for ground and excited states of ^{76}Ge and ^{82}Se nuclei. *Phys. Rev. C*, 50:R2660–R2663, Dec 1994.

[4] A. S. Barabash. Brief review of double beta decay experiments. In *Proceedings, 2nd International Conference on Particle Physics and Astrophysics (ICPPA 2016): Moscow, Russia, October 10-14, 2016*, 2017.

[5] J. Toivanen and J. Suhonen. Study of several double-beta-decaying nuclei using the renormalized proton-neutron quasiparticle random-phase approximation. *Phys. Rev. C*, 55:2314–2323, May 1997.

[6] Pekka Pirinen and Jouni Suhonen. Systematic approach to β and $2\nu\beta\beta$ decays of mass $a = 100 - -136$ nuclei. *Phys. Rev. C*, 91:054309, May 2015.

[7] J. Barea, J. Kotila, and F. Iachello. $0\nu\beta\beta$ and $2\nu\beta\beta$ nuclear matrix elements in the interacting boson model with isospin restoration. *Phys. Rev. C*, 91:034304, Mar 2015.

[8] E. A. Coello Pérez, J. Menéndez, and A. Schwenk. Gamow-teller and double-β decays of heavy nuclei within an effective theory. *Phys. Rev. C*, 98:045501, Oct 2018.

[9] A. Bakalyarov, A. Balysh, A. S. Barabash, P. Beneš, Ch. Briançon, V. Brudanin, P. Čermák, V. Egorov, F. Hubert, Ph. Hubert, N. A. Korolev, V. N. Kosjakov, A. Kovalik, N. A. Lebedev, V. I. Lebedev, A. F. Novgorodov, N. I. Rukhadze, N. I. Štekl, V. V. Timkin, I. E. Veleshko, Ts. Vylov, and V. I. Umatov. Improved limits on β- and β-β-decays of 48ca. *Journal of Experimental and Theoretical Physics Letters*, 76(9):545–547, Nov 2002.

[10] J. W. Beeman, F. Bellini, P. Benetti, L. Cardani, N. Casali, D. Chiesa, M. Clemenza, I. Dafinei, S. Di Domizio, F. Ferroni, L. Gironi, A. Giuliani, C. Gotti, M. Laubenstein, M. Maino, S. Nagorny, S. Nisi, C. Nones, F. Orio, L. Pagnanini, L. Pattavina, G. Pessina, G. Piperno, S. Pirro, E. Previtali, C. Rusconi, K. Schäffner, C. Tomei, and M. Vignati. Double-beta decay investigation with highly pure enriched ^{82}se for the lucifer experiment. *The European Physical Journal C*, 75(12):591, Dec 2015.

[11] S. W. Finch and W. Tornow. Search for two-neutrino double-β decay of ^{96}Zr to excited states of ^{96}Mo. *Phys. Rev. C*, 92:045501, Oct 2015.

[12] A. Piepke, M. Beck, J. Bockholt, D. Glatting, G. Heusser, H.V. Klapdor-Kleingrothaus, B. Maier, F. Petry, U. Schmidt-Rohr, H. Strecker, M. Völlinger, A.S. Barabash, V.I. Umatov, A. Müller, and J. Suhonen. Investigation of the $\beta\beta$ decay of 116cd into excited states of 116sn. *Nuclear Physics A*, 577(3):493 – 510, 1994.

[13] CUORE Collaboration, C. Alduino, K. Alfonso, D. R. Artusa, III Avignone, F. T., O. Azzolini, T. I. Banks, G. Bari, J. W. Beeman, and F. Bellini. Double-beta decay of ^{130}Te to the first 0^+ excited state of ^{130}Xe with CUORE-0. *arXiv e-prints*, page arXiv:1811.10363, Nov 2018.

[14] K. Asakura et al. Search for double-beta decay of ^{136}Xe to excited states of ^{136}Ba with the KamLAND-Zen experiment. *Nucl. Phys.*, A946:171–181, 2016.

[15] W. Tornow. Search for a bosonic component in the neutrino wave function. *Nuclear Physics A*, 844(1):57c – 62c, 2010. Proceedings of the 4th International Symposium on Symmetries in Subatomic Physics.